ARTICLE

BIOTECHNOLOGY and BIOENGINEERING

Visualizing and Quantifying the Differential Cleavages of the Eukaryotic Translation Initiation Factors eIF4GI and eIF4GII in the Enterovirus-Infected Cell

Yueh-Ying Hsu,[1] Yu-Ning Liu,[1] Wen-Wen Lu,[2] Szu-Hao Kung[1]

[1]Department of Biotechnology and Laboratory Science in Medicine, National Yang-Ming University, Taipei, Taiwan, R.O.C.; telephone: +816-2-2826-7034; fax: +816-2-2826-4092; e-mail: szkung@ym.edu.tw

[2]Department of Clinical Pathology, Cheng Hsin Rehabilitation Medical Center, Taipei, Taiwan, R.O.C.

Received 29 April 2009; revision received 6 July 2009; accepted 27 July 2009

Published online 4 August 2009 in Wiley InterScience (www.interscience.wiley.com). DOI 10.1002/bit.22495

ABSTRACT: Enterovirus (EV) infection has been shown to cause a marked shutoff of host protein synthesis, an event mainly achieved through the cleavages of eukaryotic translation initiation factors eIF4GI and eIF4GII that are mediated by viral 2A protease ($2A^{pro}$). Using fluorescence resonance energy transfer (FRET), we developed genetically encoded and FRET-based biosensors to visualize and quantify the specific proteolytic process in intact cells. This was accomplished by stable expression of a fusion substrate construct composed of the green fluorescent protein 2 (GFP^2) and red fluorescent protein 2 (DsRed2), with a cleavage motif on eIF4GI or eIF4GII connected in between. The FRET biosensor showed a real-time and quantifiable impairment of FRET upon EV infection. Levels of the reduced FRET closely correlated with the cleavage kinetics of the endogenous eIF4Gs isoforms. The FRET impairments were solely attributed to $2A^{pro}$ catalytic activity, irrespective of other viral-encoded protease, the activated caspases or general inhibition of protein synthesis in the EV-infected cells. The FRET biosensors appeared to be a universal platform for several related EVs. The spatiotemporal and quantitative imaging enabled by FRET can shed light on the protease–substrate behaviors in their normal milieu, permitting investigation into the molecular mechanism underlying virus-induced host translation inhibition.

Biotechnol. Bioeng. 2009;104: 1142–1152.

© 2009 Wiley Periodicals, Inc.

KEYWORDS: fluorescence resonance energy transfer (FRET); enterovirus; protease 2A ($2A^{pro}$); translation; eIF4G

Introduction

Members of the human enterovirus (EV) belong to the genus *Enterovirus*, family *Picornaviridae*, and are implicated in a broad array of human diseases. The EVs are further classified by their subgenus names as polioviruses (PV), coxsackieviruses A (CVA), coxsackieviruses B (CVB), echoviruses, and the newer numbered EVs. The *Enterovirus* genus has now been expanded to include the previously separate *Rhinovirus* genus, which consists of more than 100 serotypes of rhinoviruses (RV; Pallansch et al., 2007). EV has a single-stranded, positive-sense RNA genome, comprising the untranslated regions (UTRs) at 5′ and 3′ ends and a long open reading frame encoding a single large polyprotein. The mature, functional virus proteins are derived from a series of post-translational cleavages of the viral polyprotein by two virus-encoded proteases, 2A ($2A^{pro}$) and 3C ($3C^{pro}$). The polyprotein first undergoes an autocatalytic cleavage by $2A^{pro}$ to release the precursor to the viral capsid proteins while the majority of other cleavages of the polyprotein are catalyzed by $3C^{pro}$ (Bedard and Semler, 2004; Pallansch et al., 2007). EV $2A^{pro}$ has been classified as a cysteine protease with three critical amino acid residues comprising the catalytic core (Bazan and Fletterick, 1988; Yu and Lloyd, 1991).

Apart from the essential role in viral polyprotein processing, $2A^{pro}$ cleaves several cellular proteins, notably the eukaryotic initiation factors 4GI (eIF4GI) and its functional homolog eIF4GII (generically referred to as eIF4G) (Barco et al., 2000; Etchison et al.,1982; Gradi et al., 1998a,b; Krausslich et al., 1987; Kuo et al., 2002; Svitkin et al., 1999). The eIF4G is a component of the cap-binding complex (eIF4F), which plays a pivotal role in the interaction between capped mRNA and the 40S ribosomal

Yu-Ning Liu's present address is Prevision Medical Corp., Taipei, Taiwan, R.O.C.
Correspondence to: S.-H. Kung
Contract grant sponsor: National Science Council, Taiwan
Contract grant number: NSC 95-2320-B-010-038; 97-2320-B-010-010-MY3
Additional Supporting Information may be found in the online version of this article.

© 2009 Wiley Periodicals, Inc.

subunit, leading to the initiation of translation (Pestova et al., 2001). Cleavage of eIF4G results in the disruption of the eIF4F complex and the consequent inhibition of cap-dependent translation. Translation of uncapped viral RNA, however, remains intact and is even enhanced as viral protein synthesis is initiated internally at the internal ribosome entry segment (IRES) (Bedard and Semler, 2004; Borman et al., 1997; Lloyd, 2006; Ohlmann et al., 1996). Both eIF4G isomers share approximately 46% identity at the amino acid level and the regions that bind the translation factors in the eIF4F complex are highly conserved (Gradi et al., 1998a,b; Svitkin et al., 1999). Moreover, eIF4G cleavage by $2A^{pro}$ was found concomitant with the induction of apoptotic cell death (Buenz and Howe, 2006; Calandria et al., 2004; Deszcz et al., 2005; Goldstaub et al., 2000; Kuo et al., 2002).

Genetic and biochemical approaches have made great progress in unraveling the viral protease activity in vitro (Martinez-Abarca et al., 1993; Sommergruber et al., 1994; Yu and Lloyd, 1991); however, the milieu of EV-infected cells may not be reproduced by the in vitro technical approaches. Live cell imaging analysis should greatly mirror the intracellular condition and allow monitoring of the in vivo kinetics of $2A^{pro}$-cleaving eIF4G, thereby elucidating the mechanistic insights into the host translation shutoff caused by EV infection. Fluorescence resonance energy transfer (FRET) is one of the few that successfully permit examination of the dynamic processes of protease–substrate interactions in the living cells (Kohl et al., 2002; Tawa et al., 2001; Yang et al., 2007). FRET describes the transfer of energy from a donor fluorophore in an excited state to a neighboring acceptor fluorophore in a distance- and orientation-dependent manner. Such transfer is characterized by a reduction of fluorescence intensity of the donor fluorophore and re-emission of fluorescence at acceptor fluorophore wavelengths (Jares-Erijman and Jovin, 2003). We previously developed a biosensor cell line based on FRET for real-time measurement of the viral protease activity in vivo. This was achieved by stable transfection of HeLa cells with plasmid encoding the green fluorescent protein 2 (GFP^2) and red fluorescent protein 2 (DsRed2) FRET pair linked with the $2A^{pro}$ cleavage sites from the viral polyprotein (Hsu et al., 2007).

In the present study, we generated the fusion substrate that harbor the FRET pair embedded with the $2A^{pro}$ cleavage motif from the eIF4GI or eIF4GII. Pronounced FRETs from the fusion substrate-expressing cells were detected until the cleavages by $2A^{pro}$ in the context of virus infection. FRET was readily measured in real-time by fluorescent microscopy and in a quantitative manner by fluorometry. The FRET biosensor was adequately sensitive to distinguish the differential cleavages of both eIF4G isomers, and the results from the FRET based-assays correlated well with those from the conventional assay. The FRET disruptions were shown independent of the apoptosis or host protein shutoff caused by EV infection. We started out with enterovirus 71 (EV71), a neurological pathogen with significant increase in epidemic activity throughout the Asia-Pacific region in recent years (Palacios and Oberste, 2005), and it can be applied to other EVs tested. This FRET biosensor system was the first of such, to our knowledge, that permitted in situ mechanistic study of the host translation inhibition subject to viral protease activity within intact cells in a direct, continuous, and quantitative fashion.

Materials and Methods

Metabolic Labeling

Cells were pulse-labeled following the protocol with some modifications (Gradi et al., 1998b). HeLa cells grown on 6-well dishes were subject to infection by EV71 at a titer of 5 plaque-forming-unit (PFU)/cell per well or left mock-infected. After virus adsorption for 1 h, cells on each well were incubated with [^{35}S] methionine/cysteine (20 μCi; Redivue PRO-MIX [^{35}S] Cell Labeling Mix, Amersham Biosciences, Buckinghamshire, UK; specific activity $>1{,}000\,Ci\,mmol^{-1}$) per well for 30 min at 2 h intervals during the infection. Cells were then harvested, washed with cold PBS, and lysed with 500 μL of lysis buffer. Label incorporation was determined by quantification of trichloroacetic acid (TCA) precipitable radiation with the β scintillation counter (LSA 2900 QuantaSmart, PerkinElmer, Shelton, CT).

Plasmids

The pGR plasmid that encodes the GFP^2-DsRed2 fusion protein with the multiple cloning site in between and the zeocin-resistance gene for selection was described (Hsu et al., 2007). Two set of complementary oligonucleotides, eIF4GIwtF/eIF4GIwtR and eIF4GIIwtF/eIF4GIIwtR, that encode the $2A^{pro}$ cleavage motifs on eIF4GI and eIF4GII, respectively, were synthesized (Supplementary Table I). Two other sets of oligonucleotides, eIF4GImutF/ eIF4GImutR and eIF4GIImutF/eIF4GIImutR, that encode the corresponding mutant cleavage motifs were also synthesized (Supplementary Table I). Each set of oligonucleotides was annealed and cloned into the *Hin*dIII/*Bgl*II sites in the pGR plasmid in-frame with the GFP^2 and DsRed2 open reading frames. The resulting plasmids were referred to as pGeIF4GIwtR and pGeIF4GImutR that encode the wild-type and mutant cleavage motifs on eIF4GI, respectively, and pGeIF4GIIwtR and pGeIF4GIImutR, for those with wild-type and mutant cleavage motifs on eIF4GII. The plasmids pCMV-FLAG-2A and pCMV-FLAG-3C that bear the $2A^{pro}$- and $3C^{pro}$-encoding regions, respectively, were previously described (Hsu et al., 2007; Tsai et al., 2009). A recombinant plasmid that encodes the catalytically inactive EV71 $2A^{pro}$ ($21H \rightarrow L$) was constructed by overlap extension PCR (Ho et al., 1989; Supplementary Material). All recombinant plasmids were confirmed by sequencing.

Stable Transfection

Stable FRET cell lines, designated FRETwt1, FRETmut1, FRETwt2, and FRETmut2, were established as previously described (Hsu et al., 2007). Briefly, they were developed by transfection of HeLa cells with the pGeIF4GIwtR, pGeIF4GImutR, pGeIF4GIIwtR, and pGeIF4GIImutR plasmid, respectively, at 1.5 μg each using Lipofectamine (Gibco-BRL, Carlsbad, CA) as per the manufacturer's instructions. Each line was selected and maintained in the presence of *zeocin*.

Western Blotting

Western blot analysis was conducted following the previous report (Kuo et al., 2002). Primary antibody used was anti-eIF4GI monoclonal antibody (1:250 dilution; BD Transduction Laboratories, San Jose, CA, E46520), mouse anti-eIF4GII monoclonal antibody (1:200 dilution; Abnova, Walnut, CA, H00008672-M01), anti-EV71 VP1 monoclonal antibody (1:1,000 dilution, Chemicon International, Temecula, CA, USA, MAB979), or the living colors rabbit anti-GFP polyclonal antibody (1:1,000 dilution, BD Bioscience, Palo Alto, CA, 632459). Mouse anti-tubulin monoclonal antibody (1:10,000 dilution; Oncogene, San Diego, CA, CP06) or mouse anti-actin monoclonal antibody (1: 1,000 dilution, Chemicon, MAB1501) was used for the loading control. Horseradish peroxidase (HRP)-conjugated goat anti-rabbit antibody (1: 1,000 dilution, Santa Cruz Biotechnology, Santa Cruz, CA, sc-2004) or HRP-conjugated goat anti-mouse antibody (1: 1,000 dilution, Santa Cruz, sc-2060) was used as the secondary antibody. Proteins were detected using the Enhanced Chemiluminescence (ECL) Western blot kit (Amersham Biosciences).

FRET Imaging

Imaging process followed the previous report (Hsu et al., 2007). Briefly, an inverted fluorescence microscope (Nikon, Japan, TE200) was used with the filter sets as follows: for GFP^2 excitation at 390 nm and emission at 515 ± 15 nm; for DsRed2 excitation at 540 nm and emission at 600 ± 25 nm was used; for FRET of GFP^2 and DsRed2 excitation was at 390 nm and emission at 600 ± 25 nm. The images in 390ex/515em and 390ex/600em were superimposed to indicate the FRET ratio.

Fluorometry

Cells were washed and resuspended with PBS, and aliquoted into a black 96-well, flat-bottom microplate (NUNC, Roskilde, Denmark). Fluorescence was measured on a fluorometer apparatus (Fluoroskan Ascent type 374; Labsystems, Rochester, NY). The excitation wavelength was 390 nm (band pass of 20 nm), and the emission wavelength for the fluorophore donor (GFP^2) and acceptor (DsRed2) was 510 nm (band pass of 10 nm) and 590 nm (band pass of 14 nm), respectively (Hsu et al., 2007).

Results

Shutoff of Host Protein Synthesis Coincident With Cleavage of eIF4GII Upon EV71 Infection

Infection of poliovirus (PV) and human rhinovirus (RV) was reported to cause suppression of the de novo synthesis of host protein (Etchison et al., 1982; Gradi et al., 1998b; Svitkin et al., 1999). We thus set out to investigate if EV71 infection also leads to the effect. HeLa cells infected by EV71 were analyzed by [^{35}S]-labeling assay at various time points post-infection (p.i.), and showed that the cellular protein was progressively lowered to the levels at about 90%, 40%, and 20% at 4, 8, and 12 h p.i., respectively (Fig. 1A). The decrease in overall cellular protein was similar to those seen

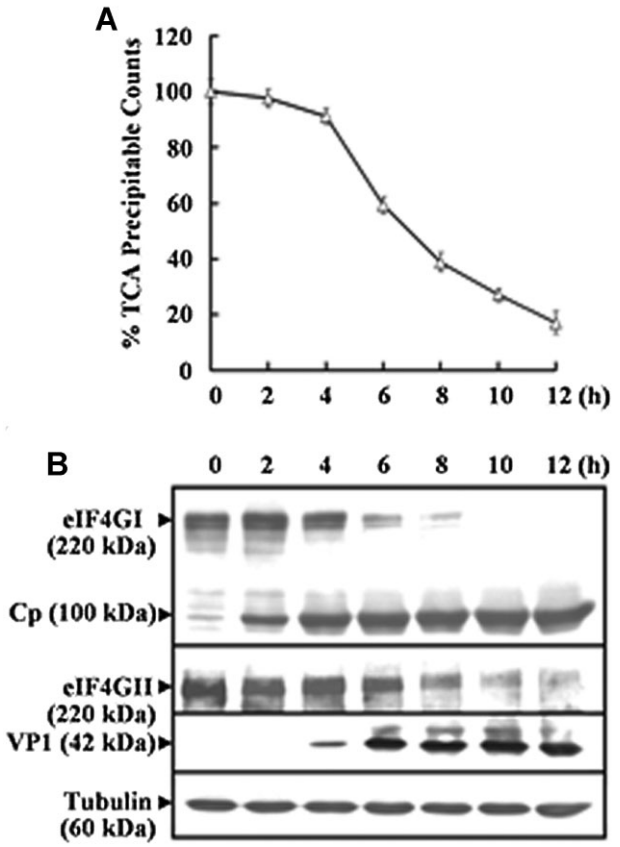

Figure 1. EV71 infection caused inhibition of host proteins synthesis with concurrent cleavages of the eIF4Gs. HeLa cells grown on 6-well dishes were infected with EV71 stock at a titer of 5 PFU/cell or left mock-infected. **A**: Cells were then labeled with [^{35}S] methionine/cysteine, withdrawn at the indicated time points, processed and subjected to β scintillation counting. % TCA precipitable counts was expressed as the radiation count of infected cells divided by that of mock-infected cell at each corresponding time point, and compared with that of the 0 h control. **B**: Cells were harvested at the indicated time points, and cell extracts were prepared and subjected to Western blot analysis for eIF4GI, eIF4GII, EV71 VP1, and tubulin. The cleavage product (C_p) of eIF4GI was indicated while that of eIF4GII was undetectable by the anti-eIF4GII antibody. Experiments were performed in triplicates with each bar representing the standard deviation (A) and a representative result shown (B). h = hour post-infection.

in the PV-and RV-infected cells where the host translation initiation factors eIF4GI and eIF4GII are cleaved (Gradi et al., 1998b; Svitkin et al., 1999); thus a relative Western blot analysis was performed on the eIF4Gs. Efficient cleavage of eIF4GI was well detectable, giving rise to a cleavage product at ca. 100 kDa; it was first detectable at 2 h p.i. and was nearly complete by 10 h p.i. On the other hand, proteolysis of eIF4GII clearly lagged behind that of eIF4GI; the eIF4GII remained intact at 4 h p.i. while it proceeded sharply to result in 15% of the level at 12 h p.i. As the infection proceeded, virus structural protein VP1 was well discernible at 4 h p.i. and reached plateau at about 6 h p.i. Cleavage of eIF4GII was concomitant with cellular protein but cleavage of eIF4GI was not (Supplementary Fig. 1), consistent with previous reports for cells infected by PV (Gradi et al., 1998b) or human RV serotype 14 (RV-14; Svitkin et al., 1999).

Generation of GFP^2–DsRed2 Expression Cell Lines

It was documented that cleavages of the eIF4GI and eIF4GII were mediated by 2A^{pro}s of some EVs and RVs with the scissile bond between the amino acids 681*682 and 699*700, respectively (Gradi et al., 2003; Lamphear et al., 1993; Sommergruber et al., 1994). To monitor the cleaving activity of 2A^{pro} for the eIF4Gs within a milieu of physiological-relevant setting, we developed an intracellular protease assay based on the principle of FRET. The recombinant construct that encodes GFP^2-DsRed2 fusion protein tethered by the 2A^{pro} cleavage motif from eIF4GI (amino acid residues 675–686) or eIF4GII (amino acid residues 693–704), namely pGeIF4GIwtR or pGeIF4GIIwtR, respectively, was generated (Fig. 2). In principle, efficient FRET should be generated due to the close proximity of GFP^2-DsRed2; the FRET is expected to be significantly reduced upon 2A^{pro}-mediated separation of the two fluorophores (Fig. 2). Moreover, the importance of residues Gly at P1′ position of the cleavage motif was previously demonstrated (Sommergruber et al., 1994); consequently, the recombinant plasmids, pGeIF4GI-mutR and pGeIF4GIImutR, each bears the mutant cleavage motif (G → R substitutions in the P1′ position) was also generated as the controls (Fig. 2). We then developed two pairs of stable cell lines designated FRETwt1/FRETmut1 and FRETwt2/FRETmut2 lines for cells transfected with the plasmids pGeIF4GIwtR/pGeIF4GImutR and pGeIF4GIIwtR/pGeIF4GIImutR, respectively (Supplementary Table II). Each line possesses relatively high FRET among the clones examined and showed comparable FRETs (as analyzed by the fluorometer assay described below). Constitutive expressions of the fusion substrate protein did not appear to affect the translation efficiency or the growth of these cells as they propagated at a similar rate as the parental HeLa cells (Supplementary Fig. 2A). They exhibited identical susceptibilities to EV71 infections as similar levels of the characteristic cytopathic effect (data not shown) and cell survival (Supplementary Fig. 2B) were seen along the infection.

Real-Time Imaging the Differential Cleavages of eIF4Gs in EV71-Infected Cells

Expression of the fluorescent substrate in the stable lines was visualized under a fluorescent microscope using the appropriate filter sets. The merged images of the uninfected cells were seen in yellow, denoting intact FRET (Fig. 3, 0 h of each cell line). The FRET stable lines were subjected to infection by EV71 stock and continuously monitored for 12 h. For the infected FRETwt1 and FRETwt2 cells, gradually enhanced GFP^2 emissions (Fig. 3A and B, panels of top rows) at the expense of FRETs (Fig. 3A and B, panels of the

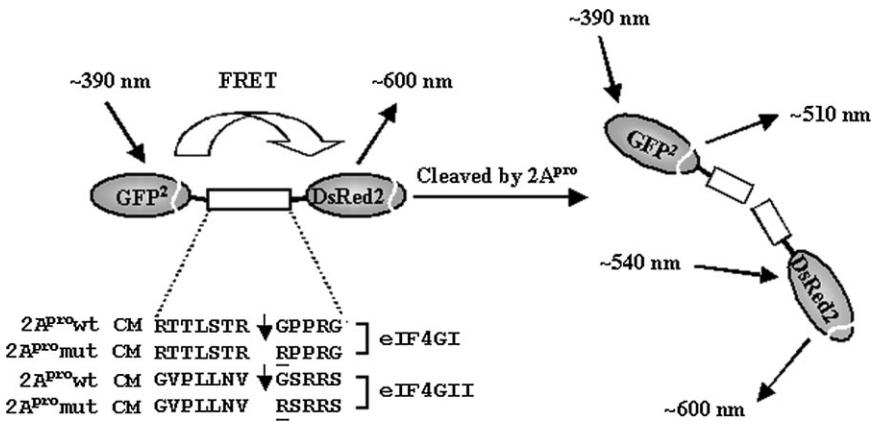

Figure 2. Schematic diagram of the principle and construct for probing the intracellular cleavages of eIF4Gs by the 2A^{pro} based on FRET. Composition of the tandem fluorophores and the key excitation and emission wavelengths for the assay are indicated. The 2A^{pro} cleavage motifs (2A^{pro}wt CM) on eIF4GI and eIF4GII, and the corresponding mutant motifs (2A^{pro}mut CM) in the linker are shown. The underlined residues represented the mutations in the P1′ positions. The arrows indicate the scissile bond of 2A^{pro}.

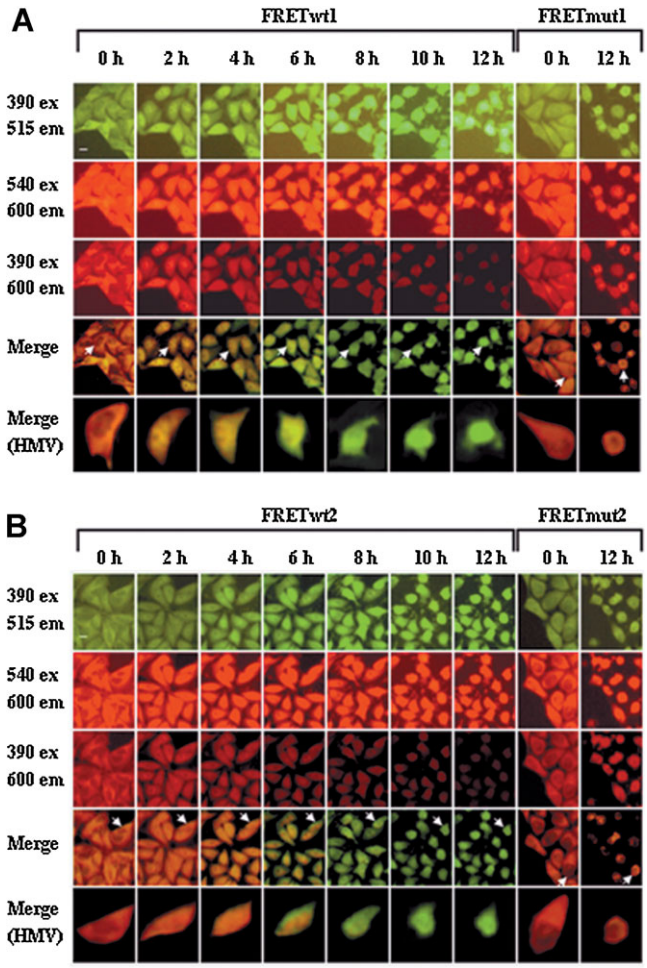

Figure 3. Imaging the kinetics of eIF4G cleavages in the infected-FRET cells. **A**: FRETwt1 and FRETmut1, and (**B**) FRETwt2 and FRETmut2 cells were infected with EV71 stock at a titer of 5 PFU/cell for 12 h. At each end point, cells were visualized by a fluorescent microscope (Nikon TE200) with 390ex/515em for GFP^2, 540ex/600em for DsRed2, and 390ex/600em for FRET. Images from the 390ex/515em and 390ex/600em were merged. High magnification view (HMV) of the cell pointed by an arrow in each merge panel was presented in the bottom rows. Bar = 5 μM. h = hour post-infection.

third row from top) with color shifting from yellow to green of the merged images (Fig. 3A and B, panels of the second rows from bottom) were observed as the infection proceeded, conceivably due to the cleavage of the fluorescent substrate in vivo by the $2A^{pro}$ activity. In contrast, no appreciable FRET abrogation was shown for the infected-FRETmut1 and -FRETmut2 cells at 12 h p.i. (Fig. 3A and B, panels of top and the third row from top), indicating high specificity exerted by $2A^{pro}$ cleaving activity in vivo. Levels of DsRed2 intensity remained constant throughout the infections for all the stable FRET cells, (Fig. 3A and B, panels of the second rows from top), thereby ruling out the possibility that host protein shutoff due to picornavirus infection could account for the FRET disruptions (Barco et al., 2000; Etchison et al., 1982; Gradi et al., 1998b). Moreover, it was noted that FRET disruption from infected FRETwt1 cells outpaced that from infected FRETwt2 cells (Fig. 3A and B, panels of the second rows from bottom), consistent with those revealed by the Western analysis (Fig. 1B and Supplementary Fig. 1). A time-lapse imaging analysis on the infected-FRETwt1 and -FRETwt2 cells was also conducted to display the continuous progression of the differential FRET disruptions at a single-cell level (Supplementary Movie). Of note was that the majority of the tandem fluorophore substrate was originally localized at the cytoplasm and then the cleavage products appeared to spread to the nucleus as the infection progressed in the FRETwt1 and FRETwt2 cells, whereas most of the fusion substrate remained localized at the cytoplasm of the infected-FRETmut1 and -FRETmut2 cells (Fig. 3A and B, panels of bottom rows; Supplementary Movie). Collectively, real-time imaging to reveal the differential kinetics of eIF4G cleavages with spatial resolution in the context of viral infection can be achieved by the FRET biosensor system.

Quantitative FRET Analyses

FRET was quantitatively measured using fluorometry, using a ratio of excited fluorescence from the acceptor molecule (DsRed2; 590 nm) divided by that from the donor molecule (GFP^2; 510 nm) both at 390 nm excitation, as an indication of FRET (Kohl et al., 2002; Tawa et al., 2001; Yang et al., 2007). The infected-FRETwt1 and -FRETwt2 cells exhibited a progressive decline at the levels of FRET ratio in a time-dependent fashion (Fig. 4A) while infection of FRETmut1 and FRETmut2 cells did not cause detectable FRET abrogation (Fig. 4B), consistent with the imaging analyses (Fig. 3). Western blot analysis was then conducted to examine if the in vivo fusion substrate was specifically cleaved upon EV71 infection. For the infected-FRETwt1 and -FRETwt2 cells, full-length fusion substrate (ca. 60 kDa) was detected only in the extracts from 0 h p.i. while the cleavage product (ca. 30 kDa) appeared in a time-dependent manner following the infections (Fig. 4C and E). On the other hand, in the infected-FRETmut1 and -FRETmut2 cells, the full-length fusion substrate remained uncleaved regardless of the infection periods (Fig. 4D and F). These data indicated that both fusion substrates were specifically cleaved on the engineered cleavage sites in the infected cells. Moreover, the FRET ratios of the infected-FRETwt1 and -FRETwt2 cells (Fig. 4A) closely correlated with the corresponding cleavage ratios of the fusion substrates ($P < 0.001$; Fig. 4C and E, below each lane) and those of the endogenous eIF4GI and eIF4GII ($P < 0.001$; Supplementary Fig. 1), suggesting that FRETwt1 and FRETwt2 cells were appropriate for the quantitative measurement of the intracellular cleaving activity of EV71 $2A^{pro}$ on the eIF4Gs. In addition, the kinetics of FRET disruption from FRETwt2 cells, but not that from FRETwt1 cells, was coincident with that of host cell protein shutoff, in line with the results from the Western blot analysis (Supplementary Fig. 1). Furthermore, to

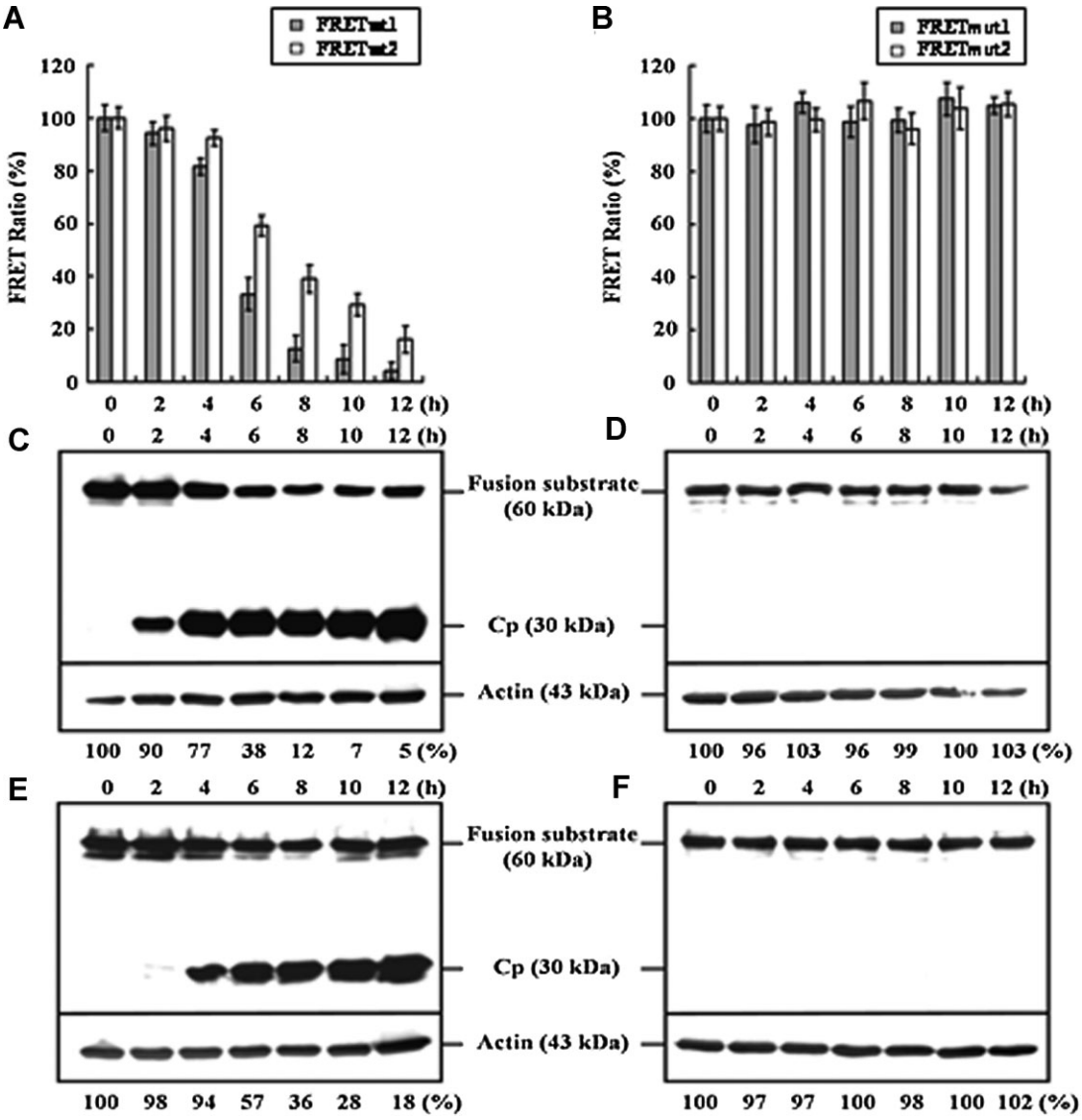

Figure 4. The quantitative fluorometry measurements correlate with the substrate cleavage ratios. **A** and **C**: FRETwt1, (**B** and **D**) FRETmut1, (A and **E**) FRETwt2, and (B and **F**) FRETmut2 cells were infected with EV71 at a titer of 5 PFU/cell, harvested at the indicated time points and subjected to (A and B) fluorometric assay with the filter sets, 390ex/510em and 390ex/590em, and (C–F) Western blot analysis with the antibody to GFP. The FRET ratio from the fluorometric assay is defined as the emission ratio of 590/510 nm with % of FRET ratio referred to as the relative value with that of 0 h control. For the Western blots, the bands corresponding to full-size of the fusion substrate (60 kDa) or its cleavage product (C_p, 30 kDa) are indicated, with the actin level used as the loading control. The substrate cleavage ratio (%) below each lane was defined as the intensity of full-length fusion substrate divided by that of the corresponding actin, and compared with that of the 0 h control. Data presented are mean values of experiments in triplicate and the bars represent the standard deviations (A and B) or a representative result for each was shown (C–F). h = hour post-infection.

evaluate the detection sensitivity of the FRET biosensors, lower titers of EV71 stock ranging from 0.04 to 1 PFU/cells were used to inoculate onto the FRET cells (Supplementary Fig. 3). The FRET disruptions were well discernible at a titer as low as 0.04 PFU/cell at 36 h or 0.2 PFU/cell at 18 h p.i. (Supplementary Fig. 3A and C) as confirmed by the Western analyses (Supplementary Fig. 3E and F). The FRET biosensors therefore served as efficient and reliable tools to quantitatively analyze the cleavage kinetics of eIF4Gs and host protein shutoff upon EV71 infection.

2A^{pro} Catalytic Activity Caused FRET Disruption

EVs carry two protease activities, namely the 2A^{pro} and 3C^{pro} (Bedard and Semler, 2004; Pallansch et al., 2007). To verify if the FRET disruptions were specifically caused by the 2A^{pro} catalytic activity, 2A^{pro}−, catalytically inactive 2A^{pro}−, 3C^{pro}-expression plasmid or empty plasmid was used to transfect each FRET cell line. FRET was significantly impaired only in the 2A^{pro}-expressing FRETwt1 and FRETwt2 cells but not in the remaining transfected-FRET

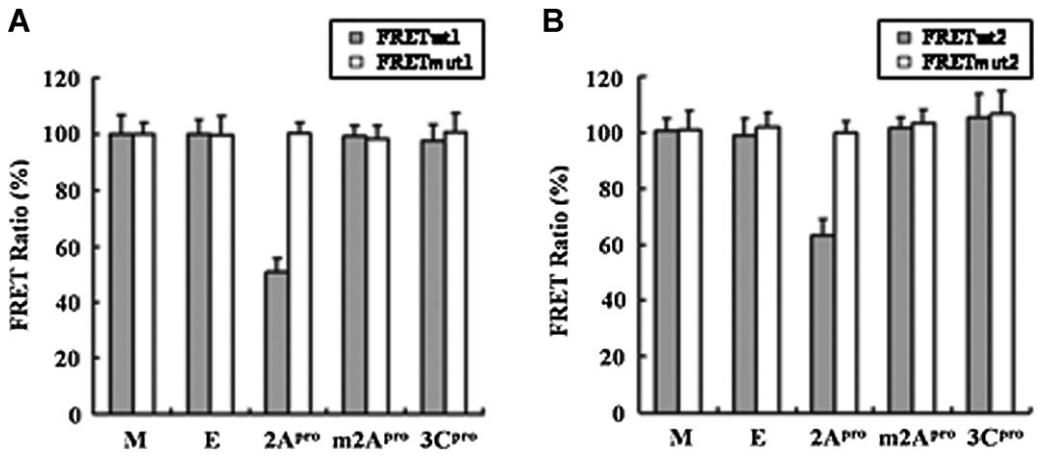

Figure 5. The $2A^{pro}$ catalytic activity was adequate to cause the FRET disruptions. **A**: FRETwt1 and FRETmut1, and (**B**) FRETwt2 and FRETmut2 cells grown on a 24-well dish were transfected with pFLAG-CMV-2 (empty plasmid), pCMV-FLAG-2A (a $2A^{pro}$ expression plasmid), pCMV-FLAG-2A(H21L) (a catalytically inactive $2A^{pro}$ expression plasmid), or pCMV-FLAG-3C (a $3C^{pro}$ expression plasmid) at the amount of 2 μg each or left-mock transfected for 60 h using the Lipofectamine method (Kuo et al., 2002). FRET ratio was determined and presented as in Figure 4. The data shown were mean values of experiments in triplicate and the bars indicated the standard deviations. M = mock; E = empty plasmid; $m2A^{pro}$ = mutant $2A^{pro}$.

lines (Fig. 5). The data indicated that catalytic activity of $2A^{pro}$ rather than $3C^{pro}$ or any redundant proteolytic activities associated with EV71 infection was responsible for the FRET disruptions.

FRET Conversion Is Independent of the Apoptosis and Translation Shutoff

To investigate if the reduced FRETs from FRETwt1 and FRETwt2 cells depend on the de novo synthesis of $2A^{pro}$ during EV71 replication, we took out $2A^{pro}$ activity upon viral infection using MPCMK (Supplementary Material), a specific inhibitor of $2A^{pro}$s of EVs and RVs (Molla et al., 1993). FRET disruptions caused by EV71 infection were significantly reversed in the presence of MPCMK in a dose-dependent manner (Fig. 6A, lanes 1–4), in line with the scenario of eIF4G cleavages revealed by Western analysis (Fig. 6B, lanes 1–4). The data support the finding that $2A^{pro}$ alone but not other virus gene products generated from EV71 multiplication is responsible for the FRET abrogation (Fig. 5). In addition, it was reported that $2A^{pro}$s of a certain EV and RV provoked caspase-dependent apoptosis (Buenz and Howe, 2006; Calandria et al., 2004; Deszcz et al., 2005; Goldstaub et al., 2000; Kuo et al., 2002), and that caspase-dependent cleavages of eIF4GI and eIF4GII were demonstrated in cells subject to the apoptotic inducer (Clemens et al., 1998; Marissen and Lloyd, 1998; Morley et al., 2005). To examine if caspase activities exert any effect on the FRET disruption, we exposed the FRET cells to the general caspase inhibitor Z-VAD-FMK (Supplmentary Material; Deszcz et al., 2004; Roberts et al., 2000) upon infection. FRET disruptions and eIF4G cleavages were not apparently eased, negating the possibility that the FRET disruptions were caused by caspases-dependent cleavages of the fusion substrates in vivo (Fig. 6A and B, lane 5). Moreover, it was shown that cleavage of eIF4G during apoptosis correlates with translation shutoff (Clemens et al., 1998; Marissen and Lloyd, 1998). To investigate if the FRET decline was secondary to apoptosis or translation shutoff, the FRET cells were treated with an apoptotic inducer cisplatin and a translation inhibitor cyclohexamide (CHX) (Supplementary Material; Fig. 6A and B, lanes 6–9). While the FRETs remained unaffected (Fig. 6A, lanes 6–9), eIF4GI was cleaved in a dose-dependent manner to give rise a band at ca. 150 kDa upon both treatments (Fig. 6B, * in lanes 6–9), a cleavage product distinct from that generated upon EV71 infection (at ca. 100 kDa) (Fig. 6B, C_p of lane 2). This was consistent with the size of the eIF4GI cleavage products generated in HeLa cells by other apoptotic inducers or in other cell types (Clemens et al., 1998; Marissen and Lloyd, 1998). On the other hand, eIF4GII remained intact (Fig. 6B, lanes 6, 8, and 9) or moderately degraded (decreased by ca. 15%) (Fig. 6B, lane 7) upon the treatments, suggesting that eIF4GII was more resistant than eIF4GI to the cleavage by the activated caspase activities upon cisplatin/CHX treatment. Taken together, the data supported the notion that the FRET decline occurred specifically upon the $2A^{pro}$ activity in the context of EV71 infection and is independent of the cellular milieu where apoptosis is undergoing or/and protein synthesis is inhibited.

General Utility of the FRET Biosensors for EVs

To test the conservation of $2A^{pro}$ activities from other EVs, a closely related EV, coxsackievirus A16 (CVA16), two slightly

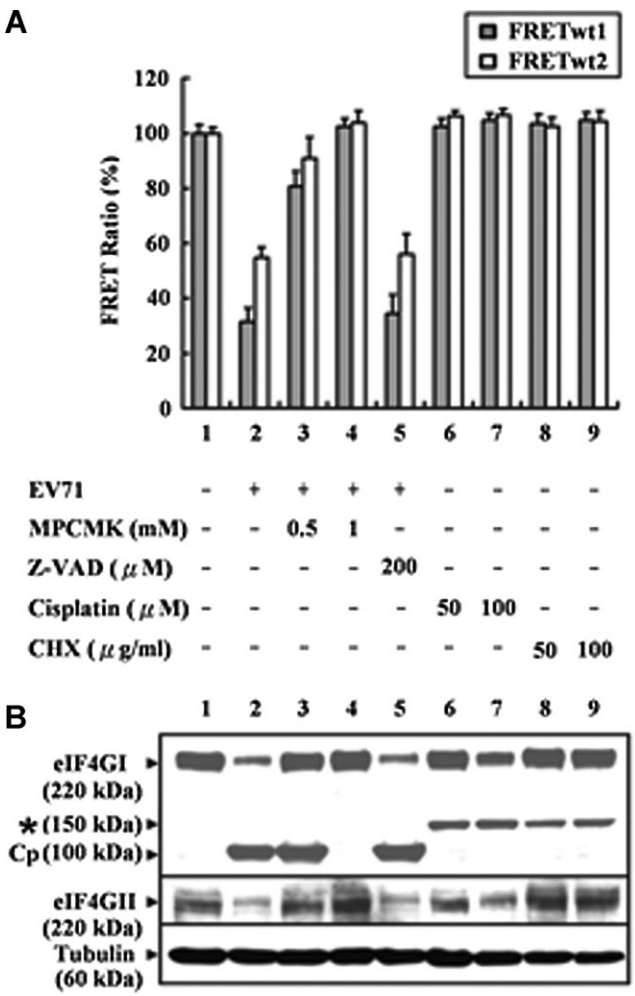

Figure 6. Apoptosis and protein shutoff do not play major roles in the FRET disruption upon EV71 infection. FRETwt1 and FRETwt2 cells grown on 6-well dishes were mock-infected (lane 1) or infected with EV71 at a titer of 5 PFU/cell (lanes 2–5) in the presence of MPCMK at 0.5 mM (lane 3) or 1 mM (lane 4), or Z-VAD-FMK at 200 μM (2 h prior to and during the infection; lane 5). The FRET cells were also treated with cisplatin at 50 μM (lane 6) or 100 μM (lane 7), and CHX at 50 μg/mL (lane 8) or 100 μg/mL (lane 9). At 6 h p.i. or post-treatment, cells were harvested and subjected to (**A**) FRET fluorometric assay and (**B**) Western blot analyses with the anti-eIF4GI and eIF4GII antibodies. Data of the FRET assay were from three separate experiments with the mean values and standard deviation shown. A representative blot was shown with the distinct eIF4GI cleavage products upon EV71 infection (C_p) and cisplatin/CHX treatment (*) indicated.

remote EVs, CVB1 and CVB4, and a phylogenetically distant virus herpes simplex virus type 1 (HSV-1), were used to infect the FRETwt1 and FRETwt2 cells. Analysis by the fluorometer assay showed that infections by either of the EV appeared to result in FRET declines as did by EV71 infection, whereas infection by HSV-1 did not cause a measurable decline in FRET (Fig. 7). Moreover, the cleavage ratios of the fusion substrate and endogenous eIF4Gs correlated closely with the corresponding FRETs, in support of the FRET biosensor system as being a universal tool for the quantitative measurements of $2A^{pro}$ activity from several EVs as a group.

Discussion

Viruses are dependent on the host cell for the translation of their mRNAs because most viral genomes do not encode any part of the translational apparatus. Consequently, many viruses have evolved diverse and elaborate mechanisms to inhibit cellular mRNA translation specifically, which in some cases may be coupled to preferential translation of viral mRNAs (Lloyd, 2006). One example of such inhibition is the mechanism by which picornaviruses target a component of the cellular eIF4F cap-initiation complex, in this case the eIF4G species proteolytically cleaved by viral $2A^{pro}$ (Barco et al., 2000; Etchison et al., 1982; Gradi et al., 1998b; Krausslich et al. 1987; Kuo et al., 2002; Svitkin et al., 1999). In view of the EV-infected cells, multifarious factors may dynamically modulate such a $2A^{pro}$-mediated proteolysis. Local $2A^{pro}$ concentration is dictated by the IRES-directed translation and the concomitant auto-cleavage from the viral polyprotein. As a consequence of the early phase of eIF4G cleavage [and other modifications (Lloyd et al., 2006)], host translation is progressively depressed and pro-apoptotic events initiated, leading to a microenvironment that can aggravate the cap-dependent translation (Barco et al., 2000; Goldstaub et al., 2000; Kuo et al., 2002; Morley et al., 2005) while favor the IRES-dependent translation and thus the generation of increasing amount of $2A^{pro}$ until reaching plateau during the viral multiplication cycle (Fig. 1B). Therefore, results obtained by the conventional end-point, in vitro approaches did not necessarily reflect what occurs in vivo; indeed, recombinant $2A^{pro}$ can only cleave the eIF4G with much less efficiency in vitro (Bovee et al., 1998; Haghighat et al., 1996). Hence, a protease assay for monitoring the eIF4G cleavage and the concurrent host translation inhibition in the context of a virus-infected cell would be desirable.

The FRET-based biosensor system, as addressed herein, appears to be a suitable tool for analysis of the in vivo proteolytic event. It allowed real-time imaging of the eIF4G proteolysis in single live cells (Fig. 3 and Supplementary Movie), which is not accessible by the traditional technologies. Complement to the imaging study lies the ability to quantitatively probe the eIF4G proteolysis of a population of cells (Fig. 4). Moreover, the resolution of the biosensor system is sufficiently high to differentiate the cleavage dynamics between the two eIF4G species. FRET decline of the EV71-infected biosensor cells resulted solely from $2A^{pro}$ catalytic activity but not from alternative proteolytic activity such as viral $3C^{pro}$ (Fig. 5) or activated caspases in the apoptotic cells (Fig. 6). Finally, all the data from the FRET-based system correlated closely with those from the reference Western analysis (Figs. 4 and 7, and Supplementary Figs. 1 and 2), making it a robust and reliable in vivo assay to dissect the cellular translation-shutoff induced by virus infection.

The primary feature of the biosensor system is its utilization of GFP^2/DsRed2 FRET pair, which makes it unique among FRET analyses. This FRET couple possess an

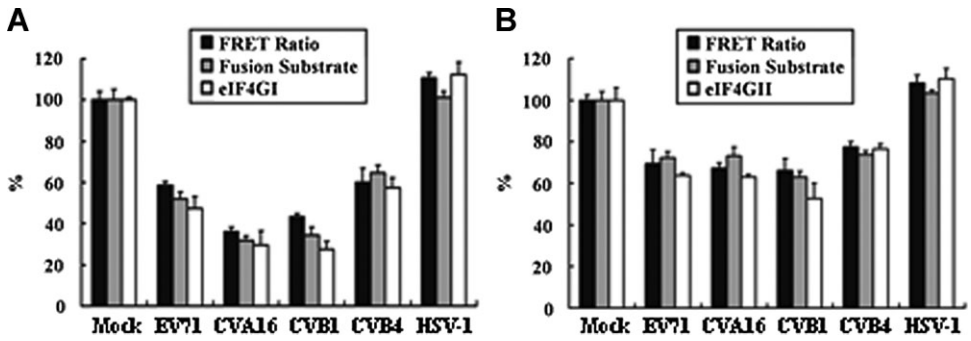

Figure 7. General use of the FRET biosensor system for EVs. **A**: FRETwt1 and (**B**) FRETwt2 cells were infected with viral stocks of EV71, CVA16, CVB1, CVB4, and HSV-1 or left mock-infected. As the infection reached ca. 75% cytopathic effect, cells were harvested and subjected to the fluorometer assay (solid bar) as well as Western blot analysis for the fusion substrates (gray bar) and the endogenous species (empty bar) of (A) eIF4GI and (B) eIF4GII. All data were analyzed and presented as those in the legends to Figures 1 and 4.

adequate spectral overlap between donor emission and acceptor absorption but separated emission spectra to permit their selective imaging (Hsu et al., 2007; Tsai et al., 2009). Based on this FRET couple, a wide detection range of EV from 0.04 to 5 PFU/cell could be achieved (Fig. 4 and Supplementary Fig. 3). The added value with the tandem fluorophore is that oligomers (at least at the size of ca. 120-kDa for a dimer) could be formed via DsRed2 oligomerization and excluded from nucleus (Campbell et al., 2002; Söling et al., 2002) until the proteolysis that permitted passive diffusion of monomeric GFP[2] into the nucleus (Fig. 3A and B, panels of bottom of rows), thereby acting as a surrogate maker for spatial resolution of FRET conversion.

Another element that constitutes the FRET biosensor is the linker in between the FRET pair. The primary sequences of the cleavage motif from each eIF4G species are critical as the distinct cleavage dynamics of the endogenous substrates are accurately modeled by the corresponding fluorogenic substrates, and it is sensitive to even one residue alteration at the P1′ position (Figs. 3–5). The specificity of the FRET biosensor was also revealed by the finding that the FRET remained intact (Fig. 6A, lanes 6 and 7) despite that the endogenous eIF4GI was reported to serve as a substrate for activated caspases when cells undergo apoptosis (Clemens et al., 1998; Marissen and Lloyd, 1998; Morley et al., 2005), and that the FRET declines did not result from general suppression of host protein synthesis (Fig. 6A, lanes 8 and 9). While the primary sequence of the cleavage motif is important, the tertiary structure of the substrate, especially the exposed and flexible region, also play critical roles in the proteolytic susceptibility (Hubbard, 1998). In this regard, the topology and accessibility of the cleavage motif embedded within each fusion substrate should also mirror that of each corresponding endogenous substrate. Collectively, the combined features of the fluorophore pair and the linker contributed to the specificity and sensitivity of the FRET biosensor system.

Both eIF4G isoforms were also susceptible to the cleavages by $2A^{pro}$s from other human EVs examined (Fig. 7), suggesting that the FRET-based biosensor represent an ideal platform for screening compounds against many EVs. This is especially promising owing to the emergence of the high-throughput imaging system with automated instrumentation (Starkuviene and Pepperkok, 2007; Vaisberg et al., 2006). Moreover, eIF4G cleavage by virus-encoded proteases are not restricted to members of genus *Enterovirus*; a number of retroviruses were also reported (Alvarez et al., 2003; Lamphear et al., 1993; Perales et al., 2003; Sommergruber et al., 1994; Ventoso et al., 2001). The precise cleavage sites of their substrates differ slightly among the various virus proteases. The scenario is complicated by the findings that while eIF4GI is a preferential substrate for $2A^{pro}$s of some EVs (as shown in this report) and human RV-14 (Svitkin et al., 1999) as well as proteases of some retroviruses including HIV (Ohlmann et al., 2002; Perales et al., 2003), both eIF4G isomers were reported to show similar susceptibilities to those of some other RVs (RV-2 and -6) and retroviruses (Alvarez et al., 2003; Gradi et al., 2003; Seipelt et al., 2000). Furthermore, other protein synthesis factors have also been shown to be substrates for picornaviral-mediated cleavages. These include eIF5B cleaved by $3C^{pro}$, and poly(A)-binding protein cleaved by both $2A^{pro}$ and $3C^{pro}$ (de Breyne et al., 2008; Kuyumcu-Martinez et al., 2002). Likewise, the known or predicted cleavage motifs of all these could be incorporated into the FRET system for testing their cleavage dynamics and correlating with their biological functions. The FRET biosensor thus would provide a framework for reanalysis of existing biochemical data or investigation into novel protease action, and greatly contribute to the elaboration of molecular mechanisms underlying the virus-induced protein shutoff.

We thank Dr. Wu-Tse Liu for offering the EV strains. This study was supported in part by Grants NSC 95-2320-B-010-038 and NSC 97-2320-B-010-010-MY3 from the National Science Council, Taiwan.

References

Alvarez E, Menendez-Arias L, Carrasco L. 2003. The eukaryotic translation initiation factor 4GI is cleaved by different retroviral proteases. J Virol 77(23):12392–12400.

Barco A, Feduchi E, Carrasco L. 2000. A stable HeLa cell line that inducibly expresses poliovirus 2Apro: Effects on cellular and viral gene expression. J Virol 74(5):2383–2392.

Bazan JF, Fletterick RJ. 1988. Viral cysteine proteases are homologous to the trypsin-like family of serine proteases: Structural and functional implications. Proc Natl Acad Sci USA 85(21):7872–7876.

Bedard KM, Semler BL. 2004. Regulation of picornavirus gene expression. Microbes Infect 6(7):702–713.

Borman AM, Kirchweger R, Ziegler E, Rhoads RE, Skern T, Kean KM. 1997. elF4G and its proteolytic cleavage products: Effect on initiation of protein synthesis from capped, uncapped, and IRES-containing mRNAs. RNA 3(2):186–196.

Bovee ML, Lamphear BJ, Rhoads RE, Lloyd RE. 1998. Direct cleavage of elF4G by poliovirus 2A protease is inefficient in vitro. Virology 245(2):241–249.

Buenz EJ, Howe CL. 2006. Picornaviruses and cell death. Trends Microbiol 14(1):28–36.

Calandria C, Irurzun A, Barco A, Carrasco L. 2004. Individual expression of poliovirus 2Apro and 3Cpro induces activation of caspase-3 and PARP cleavage in HeLa cells. Virus Res 104(1):39–49.

Campbell RE, Tour O, Palmer AE, Steinbach PA, Baird GS, Zacharias DA, Tsien RY. 2002. A monomeric red fluorescent protein. Proc Natl Acad Sci USA 99(12):7877–7882.

Clemens MJ, Bushell M, Morley SJ. 1998. Degradation of eukaryotic polypeptide chain initiation factor (eIF)4G in response to induction of apoptosis in human lymphoma cell lines. Oncogene 17(22):2921–2931.

de Breyne S, Bonderoff JM, Chumakov KM, Lloyd RE, Hellen CU. 2008. Cleavage of eukaryotic initiation factor eIF5B by enterovirus 3C proteases. Virology 378(1):118–122.

Deszcz L, Seipelt J, Vassilieva E, Roetzer A, Kuechler E. 2004. Antiviral activity of caspase inhibitors: Effect on picornaviral 2A proteinase. FEBS Lett 560(1–3):51–55.

Deszcz L, Gaudernak E, Kuechler E, Seipelt J. 2005. Apoptotic events induced by human rhinovirus infection. J Gen Virol 86(5):1379–1389.

Etchison D, Milburn SC, Edery I, Sonenberg N, Hershey JW. 1982. Inhibition of HeLa cell protein synthesis following poliovirus infection correlates with the proteolysis of a 220,000-dalton polypeptide associated with eucaryotic initiation factor 3 and a cap binding protein complex. J Biol Chem 257(24):14806–14810.

Goldstaub D, Gradi A, Bercovitch Z, Grosmann Z, Nophar Y, Luria S, Sonenberg N, Kahana C. 2000. Poliovirus 2A protease induces apoptotic cell death. Mol Cell Biol 20(4):1271–1277.

Gradi A, Imataka H, Svitkin YV, Rom E, Raught B, Morino S, Sonenberg N. 1998a. A novel functional human eukaryotic translation initiation factor 4G. Mol Cell Biol 18(1):334–342.

Gradi A, Svitkin YV, Imataka H, Sonenberg N. 1998b. Proteolysis of human eukaryotic translation initiation factor eIF4GII, but not eIF4GI, coincides with the shutoff of host protein synthesis after poliovirus infection. Proc Natl Acad Sci USA 95(19):11089–11094.

Gradi A, Svitkin YV, Sommergruber W, Imataka H, Morino S, Skern T, Sonenberg N. 2003. Human rhinovirus 2A proteinase cleavage sites in eukaryotic initiation factors (eIF)4GI and eIF4GII are different. J Virol 77(8):5026–5029.

Haghighat A, Svitkin Y, Novoa I, Kuechler E, Skern T, Sonenberg N. 1996. The eIF4G-eIF4E complex is the target for direct cleavage by the rhinovirus 2A proteinase. J Virol 70(12):8444–8450.

Ho SN, Hunt HD, Horton RM, Pullen JK, Pease LR. 1989. Site-directed mutagenesis by overlap extension using the polymerase chain reaction. Gene 77(1):51–59.

Hsu YY, Liu YN, Wang W, Kao FJ, Kung SH. 2007. In vivo dynamics of enterovirus protease revealed by fluorescence resonance emission transfer (FRET) based on a novel FRET pair. Biochem Biophys Res Commun 353(4):939–945.

Hubbard SJ. 1998. The structural aspects of limited proteolysis of native proteins. Biochim Biophys Acta 1382(2):191–206.

Jares-Erijman EA, Jovin TM. 2003. FRET imaging. Nat Biotechnol 21(11):1387–1395.

Kohl T, Heinze KG, Kuhlemann R, Koltermann A, Schwille P. 2002. A protease assay for two-photon crosscorrelation and FRET analysis based solely on fluorescent proteins. Proc Natl Acad Sci USA 99(19):12161–12166.

Krausslich HG, Nicklin MJ, Toyoda H, Etchison D, Wimmer E. 1987. Poliovirus proteinase 2A induces cleavage of eucaryotic initiation factor 4F polypeptide p220. J Virol 61(9):2711–2718.

Kuo R-L, Kung S-H, Hsu Y-Y, Liu W-T. 2002. Infection with enterovirus 71 or expression of its 2A protease induces apoptotic cell death. J Gen Virol 83(6):1367–1376.

Kuyumcu-Martinez NM, Joachims M, Lloyd RE. 2002. Efficient cleavage of ribosome-associated poly(A)-binding protein by enterovirus 3C protease. J Virol 76(5):2062–2074.

Lamphear BJ, Yan R, Yang F, Waters D, Liebig HD, Klump H, Kuechler E, Skern T, Rhoads RE. 1993. Mapping the cleavage site in protein synthesis initiation factor eIF-4 gamma of the 2A proteases from human Coxsackievirus and rhinovirus. J Biol Chem 268(26):19200–19203.

Lloyd RE. 2006. Translational control by viral proteinases. Virus Res 119(1):76–88.

Marissen WE, Lloyd RE. 1998. Eukaryotic translation initiation factor 4G is targeted for proteolytic cleavage by caspase 3 during inhibition of translation in apoptotic cells. Mol Cell Biol 18(12):7565–7574.

Martinez-Abarca F, Alonso MA, Carrasco L. 1993. High level expression in Escherichia coli cells and purification of poliovirus protein 2Apro. J Gen Virol 74(12):2645–2652.

Molla A, Hellen CU, Wimmer E. 1993. Inhibition of proteolytic activity of poliovirus and rhinovirus 2A proteinases by elastase-specific inhibitors. J Virol 67(8):4688–4695.

Morley SJ, Coldwell MJ, Clemens MJ. 2005. Initiation factor modifications in the preapoptotic phase. Cell Death Differ 12(6):571–584.

Ohlmann T, Rau M, Pain VM, Morley SJ. 1996. The C-terminal domain of eukaryotic protein synthesis initiation factor (eIF)4G is sufficient to support cap-independent translation in the absence of eIF4E. EMBO J 15(6):1371–1382.

Ohlmann T, Prevot D, Decimo D, Roux F, Garin J, Morley SJ, Darlix JL. 2002. In vitro cleavage of eIF4GI but not eIF4GII by HIV-1 protease and its effects on translation in the rabbit reticulocyte lysate system. J Mol Biol 318(1):9–20.

Palacios G, Oberste MS. 2005. Enteroviruses as agents of emerging infectious diseases. J Neurovirol 11(5):424–433.

Pallansch M, Roos R. 2007. Enteroviruses: polioviruses, coxsackieviruses, echoviruses, and newer enteroviruses. In: Knipe DM, Howley PM, editors. Fields Virology, 5th ed. Philadelphia: Lippincott Williams & Wilkins. pp 839–893.

Perales C, Carrasco L, Ventoso I. 2003. Cleavage of eIF4G by HIV-1 protease: Effects on translation. FEBS Lett 533(1–3):89–94.

Pestova TV, Kolupaeva VG, Lomakin IB, Pilipenko EV, Shatsky IN, Agol VI, Hellen CU. 2001. Molecular mechanisms of translation initiation in eukaryotes. Proc Natl Acad Sci USA 98(13):7029–7036.

Roberts LO, Boxall AJ, Lewis LJ, Belsham GJ, Kass GE. 2000. Caspases are not involved in the cleavage of translation initiation factor eIF4GI during picornavirus infection. J Gen Virol 81(7):1703–1707.

Seipelt J, Liebig HD, Sommergruber W, Gerner C, Kuechler E. 2000. 2A proteinase of human rhinovirus cleaves cytokeratin 8 in infected HeLa cells. J Biol Chem 275(26):20084–20089.

Söling A, Simm A, Rainov N. 2002. Intracellular localization of herpes simplex virus type 1 thymidine kinase fused to different fluorescent proteins depends on choice of fluorescent tag. FEBS Lett 527(1–3):153–158.

Sommergruber W, Ahorn H, Klump H, Seipelt J, Zoephel A, Fessl F, Krystek E, Blaas D, Kuechler E, Liebig HD, Skern T. 1994. 2A proteinases of coxsackie- and rhinovirus cleave peptides derived from eIF-4 gamma via a common recognition motif. Virology 198(2):741–745.

Starkuviene V, Pepperkok R. 2007. The potential of high-content high-throughput microscopy in drug discovery. Br J Pharmacol 152(1):62–71.

Svitkin YV, Gradi A, Imataka H, Morino S, Sonenberg N. 1999. Eukaryotic initiation factor 4GII (eIF4GII), but not eIF4GI, cleavage correlates with inhibition of host cell protein synthesis after human rhinovirus infection. J Virol 73(4):3467–3472.

Tawa P, Tam J, Cassady R, Nicholson DW, Xanthoudakis S. 2001. Quantitative analysis of fluorescent caspase substrate cleavage in intact cells and identification of novel inhibitors of apoptosis. Cell Death Differ 8(1):30–37.

Tsai MT, Cheng YH, Liu YN, Liao NC, Lu WW, Kung SH. 2009. Real-time monitoring of human enterovirus (HEV)-infected cells and anti-HEV 3C protease potency by fluorescence resonance energy transfer. Antimicrob Agents Chemother 53(2):748–755.

Vaisberg EA, Lenzi D, Hansen RL, Keon BH, Finer JT. 2006. An infrastructure for high-throughput microscopy: Instrumentation, informatics, and integration. Methods Enzymol 414:484–512.

Ventoso I, Blanco R, Perales C, Carrasco L. 2001. HIV-1 protease cleaves eukaryotic initiation factor 4G and inhibits cap-dependent translation. Proc Natl Acad Sci USA 98(23):12966–12971.

Yang J, Zhang Z, Lin J, Lu J, Liu BF, Zeng S, Luo Q. 2007. Detection of MMP activity in living cells by a genetically encoded surface-displayed FRET sensor. Biochim Biophys Acta 1773(3):400–407.

Yu SF, Lloyd RE. 1991. Identification of essential amino acid residues in the functional activity of poliovirus 2A protease. Virology 182(2):615–625.